Available online at www.sciencedirect.com

ScienceDirect

Proceedings of the Combustion Institute 000 (2018) 1–8

Proceedings of the Combustion Institute

www.elsevier.com/locate/proci

An experimental and numerical study of thermal and chemical structure of downward flame spread over PMMA surface in still air

O.P. Korobeinichev [a,*], A.I. Karpov [b], A.A. Bolkisev [b], A.A. Shaklein [b], M.B. Gonchikzhapov [a,c], A.A. Paletsky [a], A.G. Tereshchenko [a], A.G. Shmakov [a,c], I.E. Gerasimov [a], A. Kumar [d]

[a] *Voevodsky Institute of Chemical Kinetics and Combustion, Novosibirsk, Russia*
[b] *Udmurt Federal Research Center, Russian Academy of Science, Ural Branch, Izhevsk 426067, Russia*
[c] *Novosibirsk State University, Novosibirsk 630090, Russia*
[d] *Indian Institute of Technology Madras, Chennai 600036, India*

Received 1 December 2017; accepted 1 June 2018
Available online xxx

Abstract

This study presents the results of a comprehensive experimental investigation and numerical simulation of the downward flame spread over PMMA slabs. For the first time, in the case of downward flame spread over PMMA slab 9.6 mm thick, temperature and species concentration fields in the gas-phase flame, temperature profiles in the condensed phase and dependence of the heat flux to the burning surface on the distance from the flame front were obtained. A coupled model of heat and mass transfer involving two-dimensional elliptic conservation equations both for gas phase and solid fuel has been used with the fuel surface approximation of the samples burnout. This allowed us to state, for the indefinite intermediate mode (in terms of the sample thickness, which are not neither thermally thin nor thermally thick), a mathematical model ensuring good agreement between the experimental and calculated macro parameters of combustion. The results of comparing the experimental and calculated data allowed us to determine a number of facts, which, despite the satisfactory agreement between the simulation and the experimental data in the main macro parameters, indicate the necessity of further improvement of the model derived. Such facts are: the increasing disagreement between the calculation and the experiment in the position of the maxima of the temperature in the gas phase as the distance from the flame front grows; essential difference in the width of the MMA and O_2 consumption zone between the calculation and the experiment; identification in the experiment of CO as an intermediate product. Further improvement of the model should be aimed

* Corresponding author.
E-mail address: korobein@kinetics.nsc.ru (O.P. Korobeinichev).

https://doi.org/10.1016/j.proci.2018.06.005

at more detailed development of the combustion reaction mechanism, which should consider at least two steps.

Keywords: Flame structure; Polymethylmetacrylate; Downward flame spread; Numerical simulation; Probing mass spectrometry

1. Introduction

The propagation of diffusion flame over solid fuel's surface is certainly regarded as a basic process relating to fire initiation and growth. Among the various spatial configurations, downward flame spread over the vertical surface of solid fuel has been intensively investigated for decades, particularly due to the definite benefits provided by such a flame spread mode. From the experimentalist's view-point these are: small-scale flame, independence on the ignition technique and the steady-state regime of flame propagation, which together result in the high degree of repeatability of measurements performed by different groups. In [1,2] the flame spread rate of PMMA rods from 1.56 to 12.7 mm in diameter oriented under different angles was measured; temperature measurements inside the burning PMMA rod and on its surface were performed with thermocouples and utilized for calculating the heat flux inside and outside the sample. In [3], the flame spread rate across cast PMMA slabs 10 cm wide and from 1 to 12 mm thick was measured. In this study, the temperature fields upstream from the point of flame attachment for vertically downward burning of slabs 5.4 mm thick were measured, as well as the temperature profile on the surface of the condensed phase. In [4,5] burning of PMMA slabs from 0.32 to 2.5 cm wide and 2.5 cm thick was investigated with the method of holographic interferometry, and the heat fluxes in front of the flame edge were measured. In [6], burning of different PMMA slabs from 1.5 to 10 mm thick was investigated, and a method of measuring the inclination angle of the pyrolysis zone was proposed to evaluate the heat fluxes. The authors of [7,8] investigated the flame spread across the surface of the PMMA samples from 3 to 6 mm thick placed on a gypsum board. In [9], the flame spread rate was measured over a PMMA slab 5.4 mm thick. The downward flame spread over the vertical surface of solid fuel is usually distinguished as opposed-flow flame spread [10,11]. From the viewpoint of mathematical modeling, such a flame spread mode is associated with primary simplifications of formulation: a laminar flow assumption and a two-dimensional set of governing conservation equations may be successfully employed. The former factor is ensured by small-scale flame formed around the leading edge and generally low-level gas-phase velocity, under which the flame is able to propagate. The latter one relates to actual independence of the flame parameters upon the sample width, which has been established experimentally [3–6,12,13] for the various materials and the sample orientations if the flame spreads over a flat surface of a solid fuel sample with inhibited sides and sufficiently large width. The present level of the mathematical modeling of opposed-flow flame spread over solid fuel includes the following considerations (e.g. see [14–16] and references through there): elliptic formulation of governing partial differential equations, coupled analysis for heat and mass transfer between flame and solid fuel, finite-rate chemical kinetics both for gas-phase combustion and solid fuel's pyrolysis. Since the steady-state regime is rather typical of opposed-flow flame spread, the set of equations may be reduced to the stationary form in the coordinate system fixed on the flame front [14,15]. Here, we have decided on the unsteady formulation [16], which provides a clear interpretation of the flame spread behavior from the very beginning of ignition.

Although there are a large number of publications relating to the study of downward flame spread over PMMA, no comprehensive studies including experiments and numerical simulation considering kinetics in the gas and condensed phase have so far been conducted on PMMA slabs of various thickness (from 1 to 9.6 mm). The following parameters are to be determined: the flame spread rate, the flame structure (temperature and species concentration fields over the fuel in the gas phase), temperature profiles in the condensed phase and distribution of heat fluxes on the burning surface of the fuel along the distance from the flame front.

As noted in [17]: "*While the driving mechanism of flame spread* (over solid fuel) *has already been well established, a better understanding of the flame structure may provide useful information toward predicting spread rate, extinction, and other behaviors*". Following this remark, the present study is focused on the comprehensive experimental investigation of the thermal and chemical structure of downward flame spread over PMMA samples from 1 to 9.6 mm thick, while the theoretical part relates to the parametric numerical predictions in order to perform direct comparison of the calculated results

Please cite this article as: O.P. Korobeinichev et al., An experimental and numerical study of thermal and chemical structure of downward flame spread over PMMA surface in still air, Proceedings of the Combustion Institute (2018), https://doi.org/10.1016/j.proci.2018.06.005

with the data of the present measurements. Thus, every parameter available from the experiment has been used as input data for calculations along with up-to-date collected data on physical, kinetic and transport properties involved in the flame spread process. Finally, gas-phase and solid fuel temperature and concentrations profiles, the length of the pyrolysis zone and the flame spread rate were the points used for evaluation of the validity of the numerical results.

2. Experimental

In this study, the burning of cast PMMA slabs (manufactured by Marga Cipta brand, India) 100 mm wide, 150 mm long and 1, 2, 4.6 and 9.6 mm thick was investigated. The polymer slabs used in the experiments were long enough to allow the study of the steady-state flame propagation over PMMA samples having various thickness. The schematic of the experimental setup is shown in Fig. 1 and is described in [18].

The slabs were inserted into a thin metal frame 0.2 mm thick, to prevent flame spread over the side surfaces and to ensure even flame front spread along the center of the slab surface. The metal frame with the PMMA sample was positioned on an electronic balance to ensure measurements of the polymer's mass loss rate. The flame spread rate was determined from digital camera video recording. The slabs were ignited from the top edge with a propane-butane burner. Flame structure measurements were performed only after the flame reached the steady combustion mode, i.e. after the mass loss rate and the flame spread velocity rate became constant. The leading edge of the pyrolysis zone was considered to be the flame front. The extinguished samples were cut in the middle lengthwise to determine the cross section contour of the pyrolysis zone. To measure the temperature profiles in the condensed and gas phases of the polymer combustion, 3 thermocouples made from Pt and Pt + 10%Rh wires 50 μm in diameter were used. One thermocouple was embedded in the center of the sample and the other one was installed near its surface. To secure the position of the thermocouple inside, a groove was made on the PMMA slab surface, not more than 0.5 mm wide, which was later glued together with the thermocouple with 50% solution of PMMA in dichloroethane. The flame temperature was measured with another thermocouple made from Pt and Pt + 10%Rh wires 50 μm in diameter coated with SiO_2 layer 10 μm thick to prevent catalytic reactions on the thermocouple surface. Its design was similar to that used in [13]. A thermocouple was mounted on a 3D-scanning device, which was used to ensure programmatic movement of the thermocouple for measuring the temperature profiles in perpendicular to the slab surface in different flame zones, similarly to that described in [13]. The heat loss correction due to the radiation was calculated using Kaskan's formula [19]. Calculation of the radiation correction using Kaskan's formula and Collis' and Williams' formula used in [20] provided the same result with the accuracy of 10 K (0.6%) at the temperature 1700 K. The temperature measurement accuracy was ± 50 °C. This accuracy is the total sum of the accuracies of measuring the thermal e.m.f. (± 0.01 mV, corresponding to ± 1 degree), the accuracy in calibrating the thermocouple (± 8 degrees), the accuracy of considering the radiation correction (± 20 degrees), as well as the departure from the mean value (about 20 degrees) of the temperature measured in several experiments. The readings of all the thermocouples and of the electronic balance were made using a multichannel AD converter (E14-140-M) and were synchronized with the video recording. The chemical structure of the flame was measured using a quartz microprobe with the orifice diameter of 60 μm. The internal angle of the probe's opening at the cone base was 20 degrees. Similarly to the probe described in [13], the probe was also mounted on a 3D-scanning device. In sampling, the probe was vertically stabilized against the flame front. The gas samples were introduced into the ion source of Hiden HPR 60 mass-spectrometer and were analyzed online. For all the major species detected in the PMMA flame (O_2, N_2, C_2H_4, CO_2, H_2O, C_3H_6, CO, $C_5H_8O_2$), calibration tests were conducted, and calibration coefficients were obtained against nitrogen. The procedures of determining the mole fractions of the species is described in [21] and in the Section S2 of Supplementary Materials. The mole fractions measurement accuracy was evaluated to be 10–15% for all the compounds, except the water vapor, for which it was 20%.

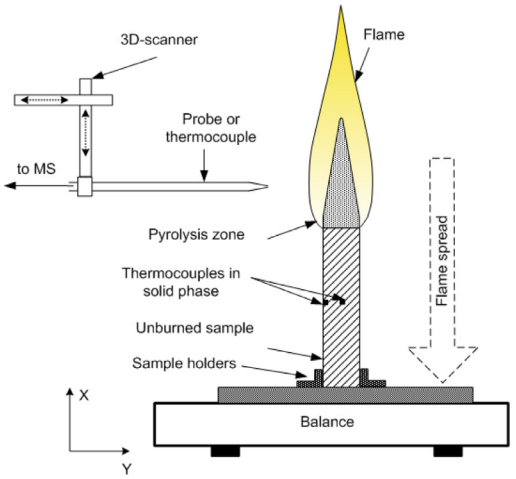

Fig. 1. Experimental setup.

Please cite this article as: O.P. Korobeinichev et al., An experimental and numerical study of thermal and chemical structure of downward flame spread over PMMA surface in still air, Proceedings of the Combustion Institute (2018), https://doi.org/10.1016/j.proci.2018.06.005

3. Mathematical model

As pointed out above, the present formulation is based on the coupled model of heat and mass transfer involving two-dimensional elliptic conservation equations both for gas phase and solid fuel under following assumptions: laminar flow, cross effects (diffusive heat transfer and thermal diffusion) are assumed to be negligible [22], and radiation is not taken into account for downward flame spread in air oxygen concentration at normal gravity [15]. Meanwhile, a test run of calculations has been carried out using the discrete ordinates method [15] in S_6 approximation, which confirmed a negligible role of radiative heat transfer for the present flame spread conditions. Nomenclature, gas-phase equations, boundary conditions and the configuration of computational domain (Fig. 1S) represented in Supplementary Materials).

Since a thermally thick layer of solid fuel is considered here, non-zero temperature gradients appear in the directions normal to the burning surface and along it, so the heat transfer in solid fuel is described by a two-dimensional elliptic equation:

$$\rho_s C_s \frac{\partial T_s}{\partial t} = \frac{\partial}{\partial x_j}\lambda_s \frac{\partial T_s}{\partial x_j} + \rho_s W_s Q_s. \quad (1)$$

In the case of a non-zero order of pyrolysis reaction, an equation for 'solid-to-gas' conversion is involved

$$\frac{\partial \alpha}{\partial t} = W_s, \quad (2)$$

where α is the conversion degree ($\alpha = 0$ stands for solid). Here W_s is the bulk reaction of pyrolysis described as

$$W_s = (1-\alpha)^n k_s \exp(-E_s/R_0 T_s), \quad (3)$$

where n is the reaction order, and the surface regression rate for every cross-section normal to the burning surface is expressed as [23]:

$$v_s = \int_{-L_s}^{0} W_s dy. \quad (4)$$

The implementation of the computational procedure was performed by an in-house code with the following major details: an implicit finite volume numerical scheme was employed; the flow field was predicted in 'pressure-velocity' primitive variables by a SIMPLE algorithm on a staggered grid; the set of quasi-linear algebraic equations was solved by the Gauss-Seidel method with an under-relaxation factor; three-point Gauss–Legendre integration was applied for calculation of the source term due to the chemical reaction; a staircase function was used to approximate the burning surface during burning out of solid fuel. Prior to comprehensive numerical studies, the series of parametric calculations have been carried out to determine proper domain size and grid resolution. The main specific factor achieved here is grid step on the burning surface in normal direction, which must be assigned at level of 0.05 mm or lower for reasonable definition of local surface parameters, mainly the conductive (gradient) heat flux.

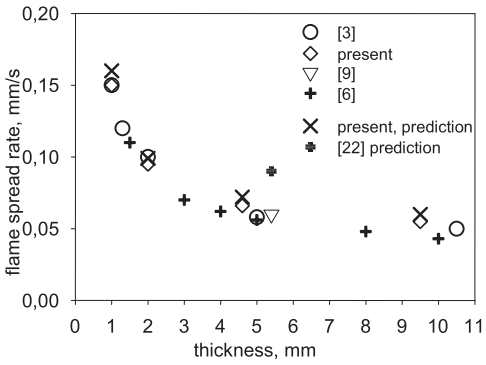

Fig. 2. Dependence of the flame spread rate on sample thickness.

The physical properties of solid fuel (PMMA) are: $\rho_s = 1160$ kg/m^3 [13], $\lambda_s = 0.188$ W/(m K) [22], $C_s = 1.01 + 0.00858\,T$ J/(g·°C) for $T < 130$°C and $C_s = 1.78 + 0.0024\,T$ J/(g·°C) for $T > 130$°C [24], $Q_s = -0.87$ MJ/kg [24]. Two sets of kinetic parameters of pyrolysis reaction were investigated: $k_s = 4.75 \cdot 10^{12}$ 1/s, $E_s = 177.6$kJ/mole, $n = 1.3$ [25], and $k_s = 2.82 \cdot 10^9$ 1/s, $E_s = 129.9$ kJ/mole, $n = 0$ [26].

The parameters of the gas-phase combustion reaction employ the heat release $Q_s = 25.9$ MJ/kg [22] and activation energy $E_g = 90$kJ/mol [22]. The pre-exponential factor was set to $k_g = 1.0 \cdot 10^8$ 1/s, which was defined through the calibrating calculations based on the comparison with experimental data of the flame spread rate (see Fig 2S in Supplementary Materials.).

4. Results and discussion

Shown in Fig. 2 is dependence of the measured and calculated flame spread rate on the sample thickness according to the data of this study and to the literature data. Our calculations presented in Figs. 2–4, 6, 7 were made using pyrolysis kinetics from [25]. In general, good agreement is observed with the experimental data available in literature.

For a PMMA slab 5.4 mm thick, the flame spread rate 0.06 mm/s, determined experimentally in [9], agrees with the data obtained in this study. In [22], calculations of the flame spread rate across a PMMA slab 4.6 mm thick were made using the pyrolysis kinetics [22,26], which provided the value of the flame spread rate of 0.09 mm/s, which is 1.5 times higher than that obtained in our measurements and in [9]. The authors of [22] compared it with the experimentally measured values obtained in [9] and that obtained according to the simplified

Please cite this article as: O.P. Korobeinichev et al., An experimental and numerical study of thermal and chemical structure of downward flame spread over PMMA surface in still air, Proceedings of the Combustion Institute (2018), https://doi.org/10.1016/j.proci.2018.06.005

Table 1
The values of the flame spread rate (u_f), the mass loss rate ($\dot{m}$), and the length of the pyrolysis zone (L_p) for samples of different thickness (h).

h (mm)	u_f (mm/s)			$\dot{m}$ (g/s)			L_p (mm)		
	Exp	Mod1	Mod2	Exp	Mod1	Mod2	Exp	Mod1	Mod2
1	0.15	0.17	0.16	0.019	0.017	0.015	1.9	1.6	1.6
2	0.095	0.131	0.10	0.022	0.026	0.026	3.1	2.9	2.7
4.6	0.065	0.076	0.072	0.037	0.059	0.036	8	8.7	7.4
9.6	0.055	0.062	0.060	0.062	0.077	0.071	18	17.8	17.7

* Mod1 - using pyrolysis kinetics [26].
** Mod2 using pyrolysis kinetics [25].

theory [27] and equal to 0.18 mm/s. Referring to [27], they believe this difference to be reasonable, considering the fact that the contribution of kinetics, with oxygen concentration being 21%, is not fully taken into account by the simplified theory and is considered only approximately by the one-step reaction in the calculations.

The measurements and the calculations of the flame spread rates u_f, of the mass burning rate $\dot{m}$ and of the length of the pyrolysis zone (the vertical distance from the flame front to the burnout point) were made for four samples of each type. Their mean values, together with the length of the pyrolysis zone L_p, are shown in Table 1. Calculation using the data [22,26] on the PMMA pyrolysis kinetics demonstrates overestimated values of the mass loss rate and of the flame spread rate. In addition, for the PMMA sample 2 mm thick, the calculated length of the pyrolysis zone turned out to be 1 mm less than the measured value. The use of kinetic parameters [25] provides better agreement with the experimental data both for the mass loss rate and the flame spread rate and for the length of the pyrolysis zone. Comparison of the calculated and measured lengths of the pyrolysis zone according to the data presented in this study and to the literature data [6] has shown their satisfactory agreement.

Figure 3 demonstrates the experimental and calculated temperature profiles in the condensed phase on the surface and in the middle of the PMMA samples of different thickness, together with the contour of the cross section of the extinguished samples. As we worked under conditions of steady flame spread, when the flame spread rate and the mass loss rate were constant, we transformed the temporal dependence of temperature in the condensed phase into the spatial dependence on the distance from the flame front x, using the experimentally measured value of the flame spread rate.

The thermocouple located on the PMMA slab surface remained in contact with the PMMA surface in the entire pyrolysis zone, and no essential shift of its position along axis x occurred. The samples of cast PMMA studied in our work did not produce an essential amount of the melt on the surface; therefore, the thermocouple was not shifted

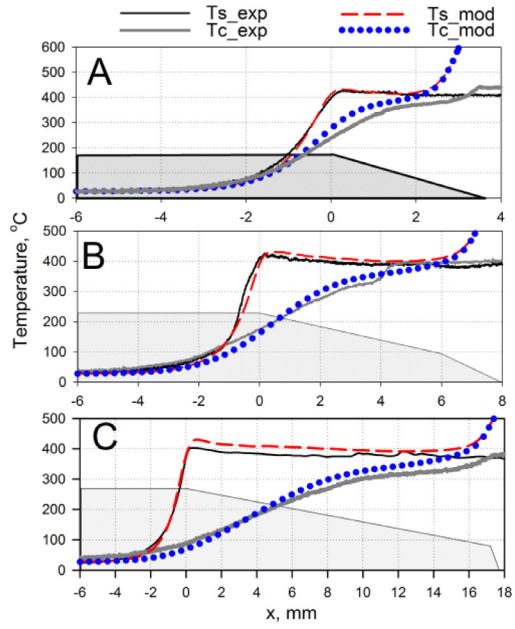

Fig. 3. Experimental and calculated temperature profiles in the condensed phase on the PMMA slab surface (T_s) and in the center (T_c) of the sample for samples of different thickness: (A) 2 mm, (B) 4.6 mm, (C) 9.6 mm.

in the pyrolysis zone due to melting of the PMMA slab.

The calculation results are in satisfactory agreement with the experimental data.

Figure 4 demonstrates experimental and calculated dependences of the temperature in the gas phase on the distance y from the centerline of the PMMA sample 9.6 mm thick measured for different distances from the flame front (x), where y is the coordinate normal to the solid fuel's surface, $y = 0$ corresponds to the middle of the sample, $x = 0$ corresponds to the flame front. The experimental contour of the pyrolysis surface is presented schematically as a shaded area. It can be seen from Fig. 4 that agreement between the calculated and experimental temperature values in immediate proximity from the flame front is satisfactory both for the

Please cite this article as: O.P. Korobeinichev et al., An experimental and numerical study of thermal and chemical structure of downward flame spread over PMMA surface in still air, Proceedings of the Combustion Institute (2018), https://doi.org/10.1016/j.proci.2018.06.005

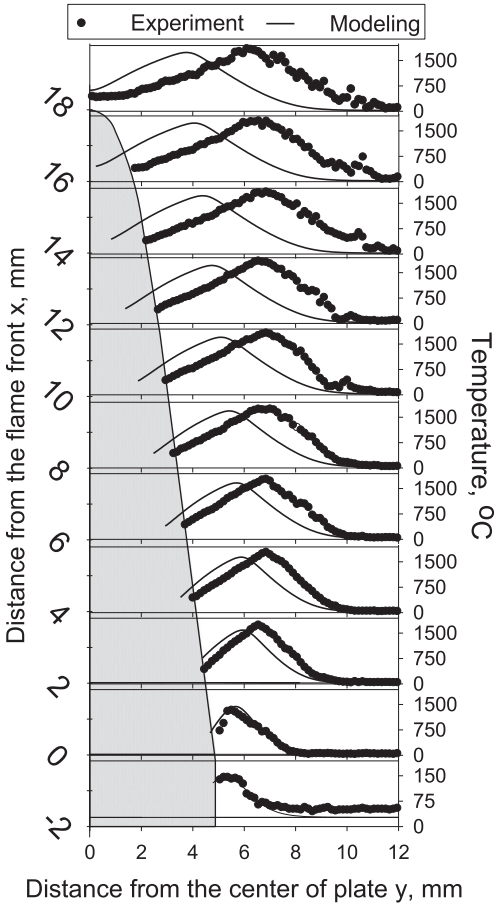

Fig. 4. Dependences of the flame temperature on the distance (y) from the centerline of the PMMA sample 9.6 mm thick measured for different distances from the flame front (x). The symbols indicate the experiment, the solid lines stand for modeling.

absolute value and for the position of the maximum. It can be seen from Fig. 4 that, as x grows, the maximum of the measured temperature and hence the heat release rate in the flame, is shifted from the fuel surface. The maximum of the calculated temperature is shifted less from the burning surface compared to the measured temperature. As in this model the gas flow is taken to be laminar, some disagreement between the modeling and experimental results in the area above the burnout point, where in the experiment visible pulsations in the flame are observed, may be expected. Two-dimensional temperature fields are provided in Fig. 3S in Supplementary Materials.

The measured temperature profiles adjacent to the burning surface (Fig. 4) were employed to calculate the temperature gradient dT/dy and to estimate the corresponding conductive heat flux from the flame zone to solid fuel. Subject to errors of

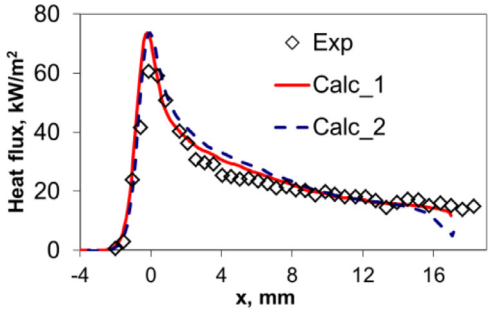

Fig. 5. Dependences of the heat flux on the burning surface along the distance from the flame front for a PMMA sample 9.6 mm thick. Symbols – experiment, lines – simulation using pyrolysis kinetics [25] (solid line) and [22,26] (dashed line).

heat flux calculation due to uncertainty in determination of the thermal conductivity of gas, the accuracy of estimating the conductive heat flux is at the level of 15–20%. Figure 5 shows good agreement between the heat fluxes calculated on the basis of the experimental data (symbols) with the heat fluxes calculated on the basis of the model (solid lines), for the PMMA sample 9.6 mm thick. In can be generally noted that the simulation data demonstrate a more expressed peak of the heat flux in the flame edge compared to the experimental data. This may be explained by the fact that in the experiment the measurement interval of the temperature field with the thermocouple was about 0.1–0.15 mm, which resulted in a slightly underestimated value of the temperature gradient. The maximum heat flux is observed close to the flame front. In the pyrolysis zone, the maximum value of the heat flux on the solid fuel's surface has been found to be 60 kW/m^2 in the experiment and ~73 kW/m^2 in the simulations. This value agrees with the data of [5,6].

Figure 6 shows experimental and modeling dependences of the species mole fractions on the distance from the centerline of the PMMA sample 9.6 mm thick measured for different distances from the flame front (x). The experimental contour of the burning surface is shown as a thin grey solid line, and the calculated surface is indicated by dashed lines. Penetration of oxygen is a key aspect which influences the burnout rate. It can be seen from Fig. 6 that at the flame front ($x = 0$), the values of oxygen concentration is essential and the gradient of MMA concentration is maximal, resulting in the maximum heat flux from the flame to the fuel surface in this area, as shown above. As x grows from 2 to 20 mm, the distance from the fuel surface at which oxygen concentration becomes noticeable increases from 2 to 4 mm. The zone of MMA consumption expands. There is disagreement between the calcu-

Please cite this article as: O.P. Korobeinichev et al., An experimental and numerical study of thermal and chemical structure of downward flame spread over PMMA surface in still air, Proceedings of the Combustion Institute (2018), https://doi.org/10.1016/j.proci.2018.06.005

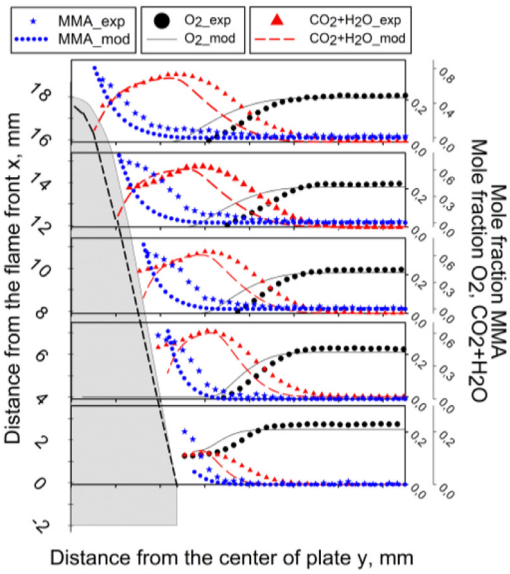

Fig. 6. Dependences of the species mole fractions on the distance from the centerline of the PMMA sample 9.6 mm thick measured for different distances from the flame front (x). The symbols indicate the experiment, the solid lines stand for modeling.

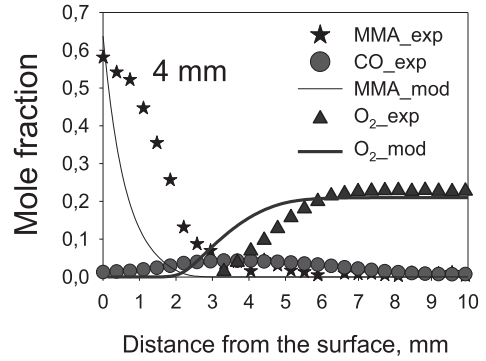

Fig. 7. Experimental and simulated dependences of MMA, O_2 and CO concentrations on the distance to the polymer surface at the distance of 4 mm from the flame front.

lated and the experimental data on the MMA concentration gradient near the fuel surface – in the experiment, the MMA gradient concentration is low, while it is high in the simulation.

Analysis of the distribution of parameters across the gas phase leads to the following conclusions. Whereas in the immediate proximity from the flame front the modeling data agree with the experimental data quite well, as the torch develops in the downstream direction, the calculated area of maximum heat release in the flame is visibly shifted to the burning surface of the solid fuel compared to the experimental data (Figs. 4 and 6). Shown in Fig. 7 are the experimental MMA, O_2 and CO mole fraction profiles measured at the distance of 4 mm from the flame front for the PMMA sample 9.6 mm thick and the calculated mole fraction profile of the gaseous fuel and oxygen used in the simulations.

First of all these data show that CO is an intermediate product of decomposition of MMA, which is the main product of PMMA pyrolysis. So processes of MMA oxidation in gas phase should consist of at least two steps, while the model includes one-step reaction. As can be seen from Fig. 7 in the modeling data the oxidation process takes place two times closer to the burning surface than in the experiment. This may be explained by the deficiency of the model utilizing a one-step reaction of MMA oxidation for the gas phase. Thus, further improvement of the model should be aimed at more detailed development of the combustion reaction mechanism, which should consider at least two steps.

5. Conclusion

Data were obtained for the flame spread rate, the mass loss rate, the length of the pyrolysis zone for samples of different thickness, the temperature profiles in the condensed phase on the surface and in the middle of the samples. For the first time, in the case of downward flame spread over PMMA slabs 9.6 mm thick, temperature and species concentration fields in the gas phase in the PMMA flame, the temperature profiles in the condensed phase and dependences of the heat flux on the burning surface along the distance from the flame front were obtained. A coupled model of heat and mass transfer involving two-dimensional elliptic conservation equations both for gas phase and solid fuel has been used with the fuel surface approximation of the samples burnout. This allowed us to state, for the intermediate indefinite mode (in terms of the sample thickness, the samples were neither thermally thin nor thermally thick), a mathematical model ensuring good agreement between the experimental and calculated temperature profiles in the condensed phase, both on the slab surface and in the slab center, as well as for most other macro parameters of combustion mentioned above.

The results of comparing the experimental and calculated data allowed us to determine a number of facts, which, despite the satisfactory agreement between the simulation and the experimental data in the main macro parameters, indicate the necessity of further improvement of the model derived. Such facts are: the increasing disagreement, as the distance from the flame front grows, in the position of the maxima of the temperature profiles in the gas phase between the calculation and in the experiment; essential difference in the width of the

Please cite this article as: O.P. Korobeinichev et al., An experimental and numerical study of thermal and chemical structure of downward flame spread over PMMA surface in still air, Proceedings of the Combustion Institute (2018), https://doi.org/10.1016/j.proci.2018.06.005

MMA and O_2 consumption zone between the calculation and in the experiment; essential concentration of CO, which is an intermediate product of fuel transformation (combustion) in the gas phase in the combustion zone, established in the experiment. These disagreements between the experiment and the simulation are due to the use of a simplified one-step model of MMA oxidation in flame. Further improvement of the model should be aimed at more detailed development of the combustion reaction mechanism, which should consider at least two steps.

Acknowledgments

This research was supported by Joint Program of the Russian Science Foundation (Project no. 16-49-02017) and Department of Science and Technology of India (Project no. INT/RUS/RSF/P-16).

The authors are thankful to Roman Glaznev for his practical contribution to the work done.

Supplementary materials

Supplementary material associated with this article can be found, in the online version, at doi:10.1016/j.proci.2018.06.005.

References

[1] M. Sibulkin, C.K. Lee, *Combust. Sci. Tech.* 9 (1974) 137–147.
[2] M. Sibulkin, J. Kim, J.V. Creeden jr, *Combust. Sci. Tech.* 14 (1976) 43–56.
[3] A.C. Fernandez-Pello, F.A. Williams, *Proc. Combust. Inst.* 15 (1975) 217–231.
[4] A. Ito, T. Kashiwagi, *Proc. Combust. Inst.* 21 (1986) 65–74.
[5] A. Ito, T. Kashiwagi, *Combust. Flame* 71 (1988) 189–204.
[6] M.B. Ayani, J.A. Esfahani, R. Mehrabian, *Fire Safety J.* 41 (2006) 164–169.
[7] J. Gong, X. Zhou, Z. Deng, L. Yang, *Int. J. Heat Mass Transfer* 61 (2013) 191–200.
[8] J. Gong, X. Zhou, J. Li, L. Yang, *Int. J. Heat Mass Transfer* 91 (2015) 225–234.
[9] M. Bundy, *Flame Tracker: Development and Testing of a New Experimental Device for Investigating Downward Spreading Flames* MS Thesis, San Diego State University, USA, 1995.
[10] I.S. Wichman, *Prog. Energy Combust. Sci.* 18 (1992) 553–593.
[11] A.C. Fernandez-Pello, *Combust. Sci. Tech.* 39 (1984) 119–134 (1984).
[12] M. Suzuki, R. Dobashi, T. Hirano, *Proc. Combust. Inst.* 25 (1994) 1439–1446.
[13] O.P. Korobeinichev, M.B. Gonchikzhapov, A.G. Tereshchenko, et al., *Combust. Flame* 188 (2018) 388–398.
[14] S. Bhattacharjee, R. Nagarkar, Y. Nakamura, *Combust. Sci. Tech.* 186 (2014) 975–987.
[15] C. Kumar, A. Kumar, *Combust. Theory Model.* 16 (3) (2012) 537–569.
[16] K.K. Wu, W.F. Fan, C.H. Chen, T.M. Liou, I.J. Pan, *Combust. Flame* 132 (2003) 697–707.
[17] S. Bhattacharjee, C. Paolini, W. Tran, J.R. Villaraza, S. Takahashi, *Proc. Combust. Inst.* 35 (2015) 2665–2672.
[18] H.R. Rakesh Ranga, O.P. Korobeinichev, A. Harish, et al., *App. Therm. Eng.* 130 (2018) 477–491.
[19] W.E. Kaskan, *Proc. Comb. Inst.* 6 (1957) 134–139.
[20] A.V. Singh, and M.J. Gollner, Combust. Flame 162(2015) 2214–2230.
[21] O.P. Korobeinichev, L.V. Kuibida, A.A. Paletsky, A.G. Shmakov, *J. Prop. Power* 14 (6) (1998) 991–1000.
[22] S. Bhattacharjee, M.D. King, C. Paolini, *Combust. Theory Model.* 8 (2004) 23–39.
[23] N.H. Kemp, *AIAA J.* 6 (9) (1968) 1790–1791.
[24] S.I. Stoliarov, R.N. Walters, *Polym. Deg. Stab.* 93 (2008) 422–427.
[25] A.Yu. Snegirev, V.A. Talalov, V.V. Stepanov, O.P. Korobeinichev, I.E. Gerasimov, A.G. Shmakov, *Polym. Deg. Stab.* 137 (2017) 151–161.
[26] G. Lengelle, *AIAA J.* 8 (1970) 1989–1996.
[27] S. Bhattachariee, M.D. King, S. Takahashi, T. Nagumo, K. Wakai, *Proc. Combust. Inst.* 28 (2000) 2891–2897.

Please cite this article as: O.P. Korobeinichev et al., An experimental and numerical study of thermal and chemical structure of downward flame spread over PMMA surface in still air, Proceedings of the Combustion Institute (2018), https://doi.org/10.1016/j.proci.2018.06.005